Contents lists available at ScienceDirect

Separation and Purification Technology

journal homepage: www.elsevier.com/locate/seppur

Flotation behavior of the most common electrode materials in lithium ion batteries

Luis Verdugo [a], Lian Zhang [a], Kei Saito [b], Warren Bruckard [c], Jorge Menacho [d], Andrew Hoadley [a],*

[a] Department of Chemical & Biological Engineering, Monash University, Melbourne, VIC 3800, Australia
[b] School of Chemistry, Monash University, Melbourne, VIC 3800, Australia
[c] CSIRO Mineral Resources, Melbourne, VIC 3169, Australia
[d] De Re Metallica Ingeniería SpA, Avda. Del Valle 576, Huechuraba, Santiago 8581151, Chile

ABSTRACT

Lithium-Ion Batteries (LIBs) are complex devices composed by different valuable and toxic materials. After use they are commonly sent to landfill, which represents a serious environment problem and wasteful due to the loss of valuable materials. At the same time these devices are highly demanded for the electronic and the electric vehicle industry. Therefore, recycling arises as a big opportunity in terms recovery of these valuable and scarce raw materials produced in specific areas of the world. For this reason, several processing technologies have been proposed to recover and recycle these materials from spent batteries. Amongst these, froth flotation technology arises as a cost-effective technology for the recovery of anodic graphite from cathode materials in spent LIBs due to the high natural hydrophobicity of graphite.

Experiments have been carried out in a 0.5 L laboratory flotation cell to demonstrate the potential of flotation as the separation process for the recycling of spent LiB materials. These experiments have focused on the separation of the binary mixtures of the three most important commercial cathode materials (LCO, NCA and NMC) and graphite and therefore simulates a completely liberated graphite/lithium metal oxide system, where the effect of organic binding materials is not present. A range of compositions, frothing agents and both collector and no collector kinetic flotation data has been obtained.

The flotation results gave a graphite concentrate with recoveries between 96.64% and 99.63% and grades between 78.13% and 90.88 %. Regarding the lithium metal oxides, these resulted in low recoveries in the concentrate between 9.47% and 16.57% and grades between 9.59% and 16.09%. A low degree of entrainment of oxide particles was achieved ranging between 0.16 and 0.29, depending on processing conditions and particle size and the best results were achieved with mixtures using NCA cathode material. These experimental results are important because they demonstrate the potential of flotation separation, but also the importance of liberation of the materials, prior to flotation.

1. Introduction

The excellent performance of Li-ion batteries (LIBs) has been a significant factor in the uptake of their use in portable electronic devices, especially personal computers, mobile phones, power tools and most recently electric bicycles and cars. Furthermore, the demand for LIBs for this e-mobility market is expected to grow rapidly to reach 2,600 GWh globally by 2030 [1]. As a consequence, production costs and prices of these devices are decreasing, but at the same time the volume of electronic waste due to LIBs is increasing at a similar rate. Traditional waste disposal via land fill or incineration is no longer appropriate due to the high content of toxic materials such as cobalt and nickel [2]. As LIBs represent up to 40 % of the total cost of an electric vehicle, it is imperative that solutions are found that involve recycling the whole battery in order to recover the individual components [3].

Fig. 1 illustrates the cathode and anode units of a lithium ion battery.

* Corresponding author at: Department of Chemical & Biological Engineering, Engineering Faculty, Monash University, 17 Alliance Lane, Clayton, VIC 3800, Melbourne, Australia.
E-mail address: Andrew.Hoadley@monash.edu (A. Hoadley).
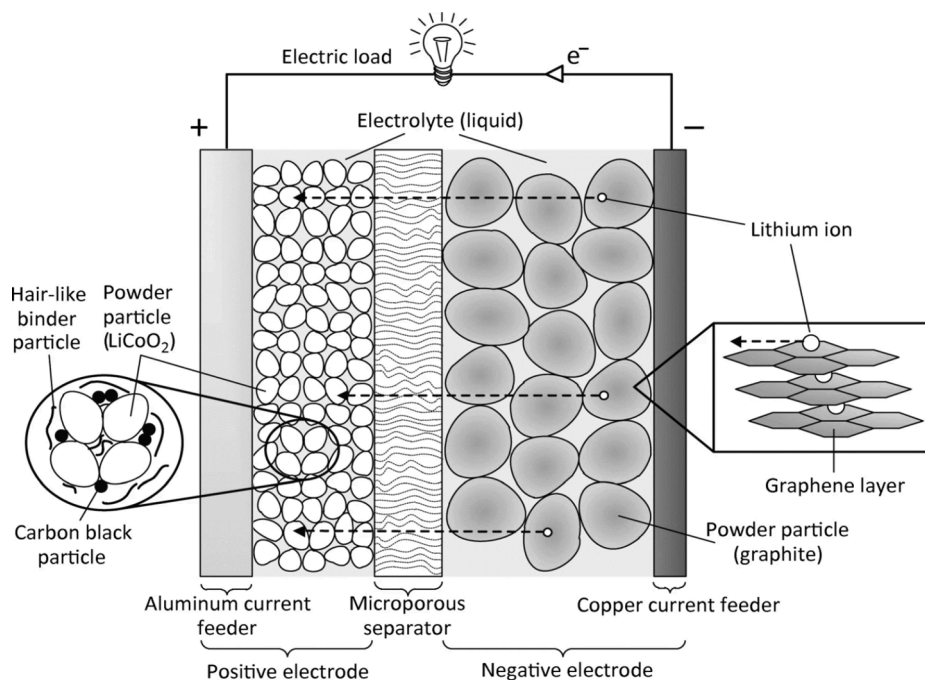
Fig. 1. Illustration of the Main Components of a Typical Lithium Ion Battery (after Vuorilehto, 2018).

The graphite and lithium metal oxides represent 22 % and 31 % of the total weight in the electrochemical unit with the copper and aluminium electrodes and plastics or metal case making up the total [4]. Graphite with a particle size distribution between 10 and 20 μm is fixed on the copper anode surface using an organic binder such as polyvinylidene fluoride (PVDF) [5]. On the cathode side, the lithium metal oxides with a particle size distribution between 1 and 17 μm [6] are fixed on the aluminium cathode surface also using the same or a similar binder.

Regarding the types or cathode chemistry used in LIBs, the most common are lithium cobalt oxide (LCO, $LiCoO_2$), lithium nickel manganese cobalt oxide (NMC-111, $LiNi_{0.33}Mn_{0.33}Co_{0.33}O_2$), (NMC-333, $Li_{1.05}(Ni_{0.33}Mn_{0.33}Co_{0.33})_{0.95}O_2$) or (NMC-441, $Li_{1.05}(Ni_{0.44}Mn_{0.44}Co_{0.11})_{0.95}O_2$) and nickel cobalt aluminium oxide (NCA, $LiNi_{0.80}Co_{0.15}Al_{0.05}O_2$), representing 91 % of the global market (Zhao et al., 2018 [7]). The last is related with specific capacity (mAh/g of cathode) of these materials used for energy storage (Nitta et Al. 2015 [8]).

In a cost point of view, anode and cathode represents the 26 % in the total cost of manufacturing and with fluctuating cost of these materials between 12 and 60 US$/kg (Gallagher et al., 2014 [9]). At the same time, due to high demand of these materials and the fluctuation of commodity prices like lithium hydroxide, graphite cobalt, nickel and manganese impacts negatively in the production costs of these cathode materials. The last suggest the importance of recycling of these materials in order to recover these valuable materials and to reduce the demand of commodities, making the battery industry more sustainable in environmental and economic terms.

Due to the importance of recovering of valuable materials from spent lithium ion batteries, in the last decade, several studies have been presented in order to recover critical materials for battery manufacturing and with a high economic value. These processes are mainly based on hydrometallurgy using acid leaching coupled with a solvent extraction process with a high efficiency but with a high acid consumption (Boxall et al., 2018 [2]) and pyrometallurgy at high temperatures which is very attractive in a process point of view due to the simplicity of the process, generating alloys of base metals directly and then recovered using a Leaching-Solvent Extraction processes (Gaines et al., 2011 [10]), but the environmental impact is serious due to generation of very toxic organic compounds such as dioxins and economic due to the intensive use of energy in the process (Winslow et al., 2018 [11]).

A part of hydrometallurgical and pyrometallurgical technologies mentioned above, froth flotation arises as an attractive, low-cost and suitable technology for separating the battery materials due to the high inherent hydrophobicity of graphite and the significant density difference between graphite and the cathode materials [12].

In the current literature, several works have been reported using flotation as a promising treatment technique for the separation of graphite from lithium metal oxides (LMO). Several authors report a high grade of lithium metal oxides (ranging between 50 % up to 95 %) in tailings and graphite grade between 80 % and 90 % in concentrates, depending on processing conditions and number of flotation stages [12,37–40]. All of these works used industrial electrode materials where there was not often full liberation and/or full binder removal. It is hypothesized that the effectiveness of flotation as a separation process for spent battery material depends on the ability to liberate the material from the binder and electrodes.

For this technology the PVDF binder material is a key aspect of treating the spent battery material. Different pre-treatment techniques have been considered such as roasting at temperatures between 500 °C and 700 °C in an inert atmosphere such as nitrogen or argon to decompose these organic coatings [13]. Other techniques include the use of organic solvents such as *N*-Methyl-2-Pyrrolidone (NMP) or Dimethylformamide (DMF) which dissolve the organic coatings thus providing an exposed metal oxide surface, the use Fenton's reagent or use of low temperatures in order to break the organic binder [14].

Additionally, in any solid–liquid separation of graphite and lithium metal oxides, the physicochemical properties of the oxides play an important role in the separation strategy. This is because these materials generate highly alkaline solutions due to the reaction with water molecules forming hydroxyl ions. This phenomenon can be explained using the Parks' approach for oxide minerals [15] and adapted and simplified to these synthetic oxides using the following chemical equilibria (Eqs. (1)–(3)).

$$LiMO_{2(s)} + 2H_2O \rightleftarrows^{k_1} LiM(OH)_{4(aq)} \tag{1}$$

$$LiM(OH)_{4\,(aq)} \leftrightarrows^{k_2} LiM(OH)_{m\,(aq)}^{4-m} + (4-m)OH_{(aq)}^- \tag{2}$$
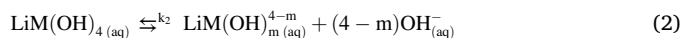
Table 1
Properties of Chemicals Used in Flotation Trials.

Reagent	Type	Chemical Formula	Density, g/L (20 °C)	HLB [25], [–]	CCC$_{95}$, mg/L [24,25]	Solubility in water, mg/L (20 °C)
2-Octanol	Frother	$C_8H_{18}O$	0.82	5.10	8.10	1,120
Aerofroth-88®		$C_8H_{18}O$	0.83	5.60	16.60	1,100
MIBC		$C_6H_{14}O$	0.81	6.00	10.70	15,000
Kerosene	Collector	N/A	0.80	14.00	N/A	Insoluble

N/A: Not available.
CCC: Critical coalescence concentration.
HLB: Hydrophilic Lipophilic Balance.

$$\text{LiM(OH)}_{m\ (aq)}^{4-m} \underset{}{\overset{k_3}{\leftrightharpoons}} \text{LiM(OH)}_{m\ (Surf)}^{4-m} \tag{3}$$

where M is the metal cation in the oxide with a total valence of +3, k_1, k_2 and k_3 are the equilibrium constants for hydrolysis of each species in solution, and m is the number of molecules involved during the reaction. From these equations it should be noted that the higher the pH (more alkaline conditions), the lower is the hydrolysis degree of these materials, which potentially can lead to a higher recovery of metal oxide particles (as there is more to potentially recover). This is also confirmed by measurement of the surface electric charge by zeta potential analysis [16].

Particle size also plays an important role in the separation of graphite-lithium metal oxides mixtures by flotation. Ultrafine oxide materials (particles with a size <10 μm) have a low probability of collision with a bubble (Trahar et al. 1976) [17]. However, they still tend to be found in the concentrate, because they can be entrained due to their small size (Shahbazia et al., 2010) [18]. This phenomenon is quantified using the entrainment factor of fine particles (Kirjavainen, 1992 a, b [19,20]), which is mainly controlled by water recovery rate, slurry viscosity, particle mass and the shape factor.

The aim of this study is therefore to determine the flotation separation performance when the materials are fully liberated. This can then be used to determine the effectiveness of liberation in the case of spent LIB material. In this study pure graphite and pure LIB cathode materials are mixed in a clean system and then separated using flotation. The three most common cathode materials currently used in LIBs were each tested individually to determine whether there are significant differences relating to the cathode chemistry.

This paper also aims to determine the best flotation parameters based on a laboratory scale Denver Cell in terms of the collector reagent, frother type, entrainment contribution, and flotation time and provide data on flotation kinetics, which can be used for process design.

2. Experimental

2.1. Materials and methods

For these experiments the following cathode materials were used, lithium cobalt oxide (LCO, LiCoO$_2$), (>99.50 % purity, density = 4.79 g/cm^3, D$_{50}$ = 5–7 μm, MSE supplies, USA), lithium nickel manganese cobalt oxide (NMC-111, LiNi$_{0.33}$Mn$_{0.33}$Co$_{0.33}$O$_2$), (>99.00 % purity, density = 4.64 g/cm^3, D$_{50}$ = 7.5 μm, MSE supplies, USA) and lithium nickel cobalt aluminium oxide (NCA, LiNi$_{0.80}$Co$_{0.15}$Al$_{0.05}$O$_2$), (purity > 99.00 %, density = 4.45 g/cm^3, D$_{50}$ = 12 μm, MSE supplies, USA). Regarding the anode material pure graphite (Gp) was used (>99.9 % purity, particle size 100 % <20 μm, Sigma-Aldrich, Australia).

The pH was adjusted using HCl solutions 0.100 M and NaOH solutions 0.100 M. These solutions were prepared and stocked in 1L volumetric flasks. A pH-meter, Hanna Instruments, model HI-98100 was used to measure pH values.

The lithium concentration in aqueous solutions was measured using Inductively Coupled Plasma (ICP) in combination with Optical Emission Spectrometry (ICP-OES) using an ICP-OES analyser (Model: iCAP^{TM} 7000 ICP–OES, provided by Thermo Fisher, USA) and using lithium

Table 2
Processing Conditions Used in Flotation Trials.

Processing Condition	Units	Value
Cell Volume	L	0.50
Agitation Speed	rpm	900
Solid Content, C$_w$	%	13
Collector Dosage	g/t	350
Frother Dosage	mg/L	30
Air Flowrate	L/h	160
Cell Area (Cross section)	cm^2	42.33

reference standards between 1.00 and 5.00 mg/L.

In the flotation experiments, kerosene, (reagent grade, Sigma-Aldrich, Australia), was used as collector for graphite in some of the experiments. The frothers evaluated in this study were 2-Octanol, supplied by Sigma-Aldrich Australia, 4-Methyl-2-pentanol (MIBC) reagent grade, 98 % purity, supplied by Sigma-Aldrich, Australia and Aerofroth® 88, (2-ethylhexanol, >99 % purity), supplied by Solvay Australia.

Tables 1–2 detail the main reagent properties and the flotation conditions used in the experiments which were kept constant for each experiment. For each experiment the collector reagent dosage was set at 350 g/t, the solid content at 13 %, the superficial gas rate at 1.05 cm/s, and the stirring speed at 900 rpm based on previous works [34,40]. The frother dosage was set at 30 mg/L in the slurry, using the critical coalescence concentration (CCC95) as reference for each frother in a concentration where the surface tension is stable (Zhang, et al, 2012 and Kowalczuk, 2013) [23,24].

2.2. Chemical characterisation of cathode materials

The natural pH and lithium concentration of slurries (at 1 % solids content) for each electrode material was determined in order to verify the alkalinity and lithium solubility of these electrode materials.

2.3. Froth flotation procedures

A Denver 0.5 L cell was used for the flotation tests, using air as the carrier gas delivered at 180 L/h equivalent to a 1.05 cm/s superficial gas rate. The mixing speed was 900 rpm, a level thought sufficient to minimise the hydrodynamic effects of entrainment of metal oxides.

For each flotation test, 76 g of mixture (graphite/oxide), in different graphite/oxide compositions between 20/80 wt% and 80/20 w% and with the main experiments using the composition 47 % graphite and 53 % oxide. They were placed in a 0.5 L laboratory-scale flotation cell (Lab Denver Cell, Laboratory XFD-12 Flotation Machine, China), together with 0.5 L of milli-Q water. The solid-water suspension (at 13 % solids content) was stirred at 900 rpm for 10 min in order to equilibrate the hydrolysis of oxides. After that a 0.100 M NaOH solution was added dropwise until adjust the suspension pH to pH 12 in order to standardise and assure the reliability of all the experiments. The slurry was then conditioned for 5 min. All the experiments were carried out at 2 conditions, the first condition was a blank or collectorless flotation experiments, aimed to study the natural flotation of graphite from the oxides
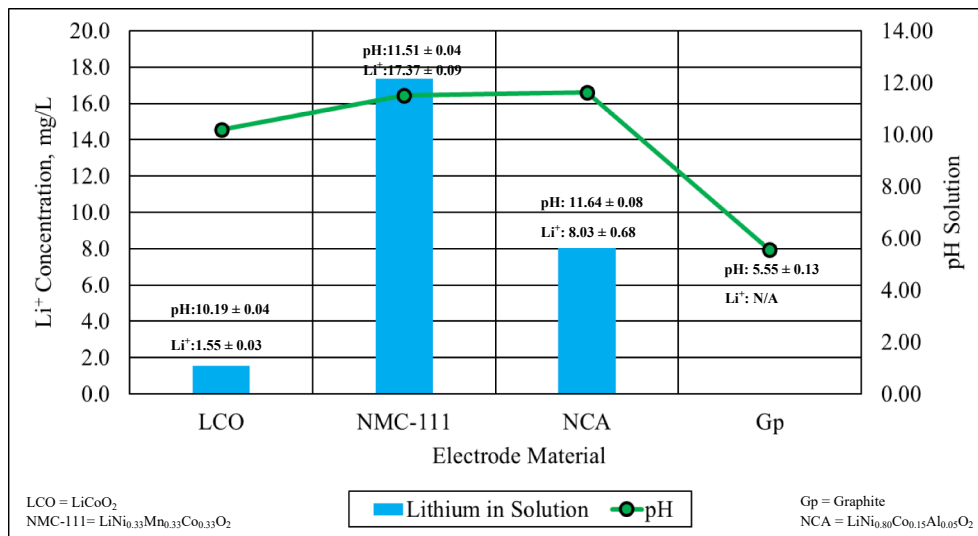
Fig. 2. Natural pH of Cathode Materials in a 1% Solids Slurry.

without collector. The second set of experiments was performed using kerosene as collector at 350 g/t, allowing 4 min of conditioning under stirring. Finally, 2-Octanol, MIBC or Aerofroth® 88 (frother) were added in order to give a 30 mg/L frother concentration in the cell, followed by two minutes of conditioning. Then, air was fed to the flotation cell at a flowrate of 180 L/h or 1.05 cm/s as superficial gas rate, marking the beginning of the flotation experiment.

After about ten seconds of air flowing, the froth became stable and the froth was recovered using a manual skimmer over 6-time intervals (0.5 min, 1 min, 2 min, 4 min, 6 min and 8 min) for a total flotation time of 8 min. The recovery process was manual, skimming every 5 s for all experiments. The collection of timed concentrates enables calculation of important flotation kinetics data. Milli-Q water at pH 12 with 30 mg/L of frother was added into the flotation cell as needed to maintain a set pulp level in the cell. Each froth fraction was recovered (6 flotation concentrates and 1 tailing) and dried at 110 °C for 18 h in a convection oven (Binder Model M 53, Germany) prior to preparation for chemical analyses.

2.4. Characterization of the flotation products

The flotation products were recovered, dried and then weighed, also the carbon composition for binary mixtures of graphite/lithium metal oxides was determined using elemental analysis in order to estimate the composition of total carbon as graphite. These analyses were carried out using a FlashSmart EA CHNS analyser, provided by Thermo Fisher Scientific, Serial Number 2019.FLS0150, Germany. These analyses were carried out at 950 °C using helium as gas carrier and oxygen as oxidant, and the reference material for these analyses was the organic compound 2,5-bis(5-*tert*-butyl-2-benzoxazolyl) thiophene (BBOT), Analytical Standard, Elemental Microanalysis, United Kingdom.

2.5. Flotation data processing methodology

Based on the mass recovered and grades of carbon and metal oxides in the feed, concentrates recovered (at 0.5, 1.0, 2.0, 4.0, 6.0 and 8.0 min) and tailings, the flotation kinetics (cumulative recovery versus time), cumulative grade, cumulative separation efficiency, degree of entrainment and selectivity index were calculated for each flotation test. The main formulas used for these calculations are as follows.

(a) Cumulative Recovery (R) [21]:

$$R = 100 \left(1 - \frac{\sum_{i=1}^{n} m_i G_i}{m_f}\right) \qquad (4)$$

where m_i is the mass of concentrate recovered at time t and G_i is the grade reported in concentrate at time t, n is the number of samples collected and m_f is the mass of pure material in feed.

(b) Cumulative Grade (G) [21]:

$$G = 100 \frac{\sum_{i=1}^{n} m_i G_i}{\sum_{i=1}^{n} m_i} \qquad (5)$$

where m_i is the mass of concentrate recovered at time t and G_i is the grade reported in concentrate at time t and n is the number of samples collected.

(c) Cumulative Separation Efficiency (SE) [21]:

$$SE = 100 \frac{m}{f(m-f)} \sum_{i=1}^{n} C_i(c_i - f) \qquad (6)$$

where m is metal content in mineral (%), f is metal content in feed (%), C_i is the fraction of the total feed weight that reports to the concentrate, n is the number of samples collected and c_i is the metal content in concentrate.

(d) Degree of Entrainment (X_i) (Savassi, 1998) [22]:

$$X_i = \frac{E_i C_W}{W_i C_m} \qquad (7)$$

where E_i is mass of oxide in the concentrate (g), C_w is the water concentration in pulp (g/L), W_i is the mass of recovered water in concentrate (g) and C_m is the concentration of solids in pulp (%).

(e) Selectivity Index (SI) (Xu, 1998) [26].

A first-order flotation kinetic model was used as basis to calculate the selectivity index. In this case a kinetic model with a modified rate constant was used (Agar et al. 1983) [27].

$$R = RI[1 - \exp(-k(t + \theta)] \qquad (8)$$

where R is the recovery at time t, RI is the ultimate recovery, k is the first-order rate constant, t is the flotation time and θ is the time
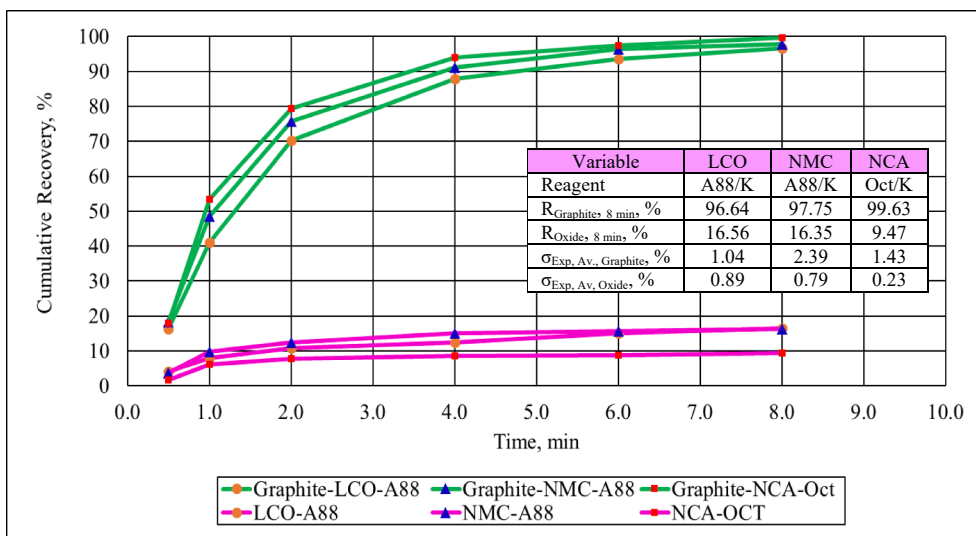
Fig. 3. Flotation Kinetics of Graphite and Oxides for Each Frother Tested.

correction factor.

After obtaining these kinetic parameters, the selectivity index is defined as the ratio of the modified rate constant of mineral A over mineral B in the flotation system, that is:

$$SI = \frac{K_A}{K_B} = \frac{RI_A k_A}{RI_B k_B} \qquad (9)$$

where RI is the ultimate recovery for each mineral (A, B), k is the kinetic rate constant for the materials studied (A, B), A is the (valuable) mineral of interest, and B is the gangue.

3. Results

The results first report the differences and similarities between the three cathode materials. These include flotation experiments, which in the first set did not a collector reagent and in the second set did use kerosene as the collector at a dosage of 350 g/t (as presented in Table 2). Both sets of results are similar and are presented in the Supplementary File. In order to reduce the length of the paper, only the results using the collector reagent are presented in this section. These experiments were conducted with a composition of 47 wt% graphite /53 wt% Lithium

metal oxides. This composition is a bit different to typical graphite and Lithium metal oxides, which is closer to 40/60 wt%. However, the second section reports the influence of composition. This section is only for the NMC materials and used the best flotation conditions that were obtained in the first set of experiments.

3.1. Characterization of cathode materials

Fig. 2 shows the natural pH of the LIB cathode materials and also graphite. These results indicate a high alkalinity for each oxide tested, which relates to the hydrolysis of these oxides in aqueous media (see Eqs. (1)–(3)). This phenomenon takes place through the leaching of lithium ions in water for each cathode material [28,29]. Therefore, a high pH value (above the natural pH) during flotation minimizes the degree of hydrolysis and can potentially improve the separation between graphite and the oxides. Regarding the dissolved lithium shown in Fig. 2, the largest concentration is NMC, which is nearly an order of magnitude higher than LCO. The dissolved lithium represents a loss of a valuable component and also a potential problem for the treatment of any wastewater.
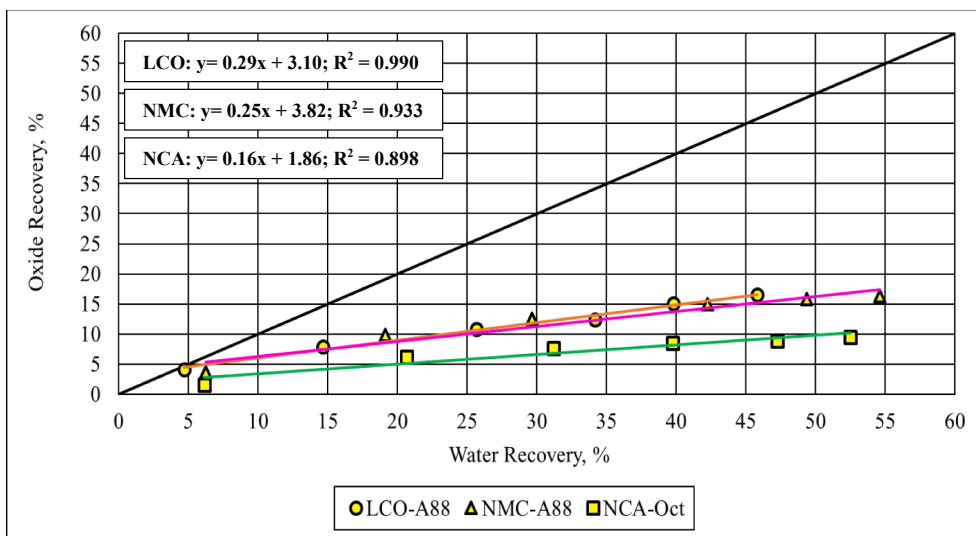
Fig. 4. Entrainment Plot for Flotation Tests Using Different Frothers.
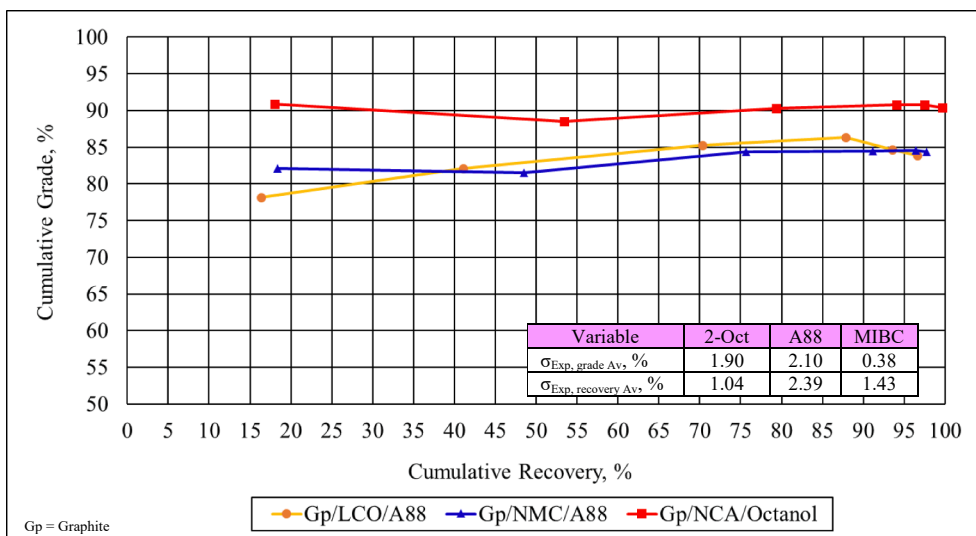
Fig. 5. Cumulative Recovery versus Cumulative Grade for Graphite Concentrates from Flotation Tests Using Different Frothers.

3.2. Flotation trials for synthetic mixtures of graphite and lithium metal oxides

3.2.1. Flotation trials with different lithium metal oxides

In these series of experiments the composition of the material being separated is constant. Fig. 3 show the component recovery as a function of flotation time for the binary mixture 47 wt% graphite and 53 wt% metal oxide. Each flotation tests uses a collector reagent and compares three different frothing agents. Fig. 3 shows a high recovery for graphite (green lines) for up to eight minutes of flotation for each mixture with a low content of oxide (pink lines) in the concentrate. The vertical separation of the two sets of lines (graphite and oxides) indicates good separation efficiency. Each pair of lines is the average of at least two duplicate experiments. From these results, the mixture of graphite/NCA using 2-octanol as frother is highlighted with the fastest kinetics, highest graphite recovery and the lowest oxide content in the concentrate. In contrast the mixture graphite/LCO has slightly slower kinetics, but still a good separation. These results suggest that all oxides tested present a similar flotation behavior. In terms of reliability of these experiments, low values of average standard deviation (σ_{Exp}) for graphite and oxides given in the table inset indicates a good reliability for all the experiments.

Fig. 4 shows a plot of the oxide recovery versus the water recovery for the same set of experiments. This figure is known as an entrainment plot. If the oxides were completely entrained in the water which is collected, then the oxide recovery would correlate directly with the water recovery and the points would lie along the 45° line. These results indicate a type 5 (linear shifted up) entrainment curve based on Konopacka's analysis for entrainment separation curves (Konopacka et al., 2010) [30].

Additionally, these results show a low degree of entrainment, which is represented by curves significantly below the identity line, with NCA showing the lowest entrainment. Given the particle size of the metal oxides used in this work this is a positive result.

Fig. 5 shows the cumulative grade versus cumulative recovery for the concentrate for the above flotation tests. This plot indicates a highly efficient separation between graphite and lithium metal oxides, where high grades are achieved after eight minutes of flotation. From these results the mixture of graphite and NCA cathode material is highlighted as the most promising option with a high content of graphite in concentrates (>90 % grade).
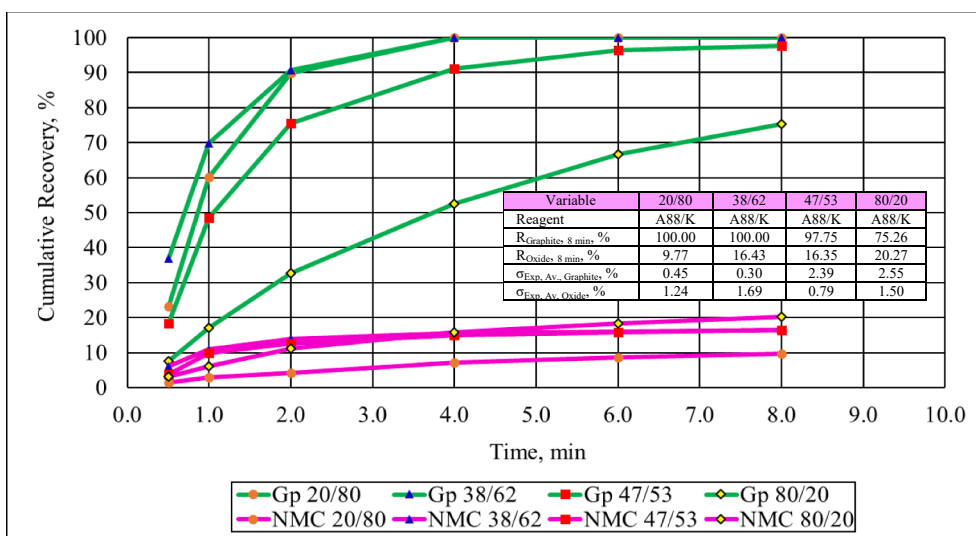
Fig. 6. Flotation Kinetics of Graphite and Oxide at Different Compositions Tested. (Using NMC-111 Cathode Material and A-88 as Frother).
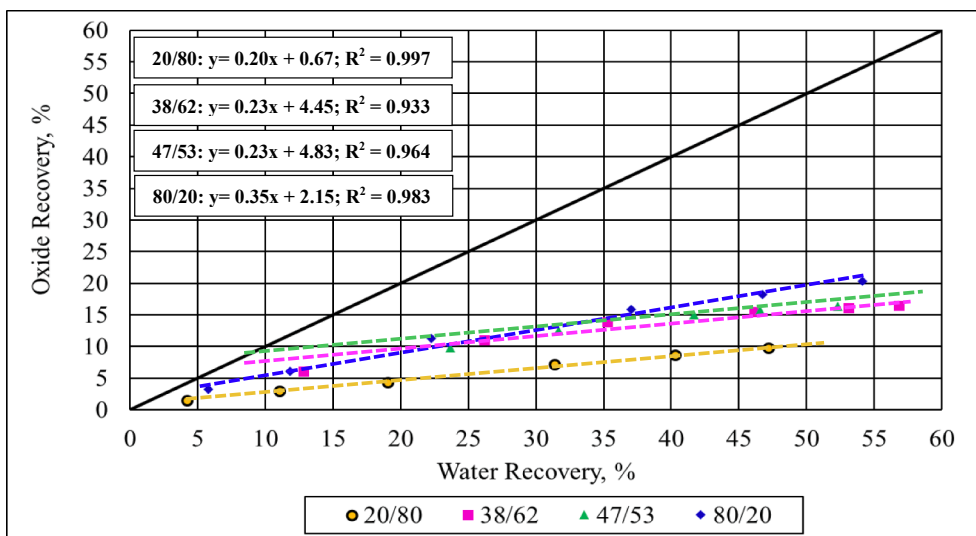
Fig. 7. Entrainment Curve at Different Compositions Tested. (Using NMC-111 Cathode Material and A-88 as Frother).
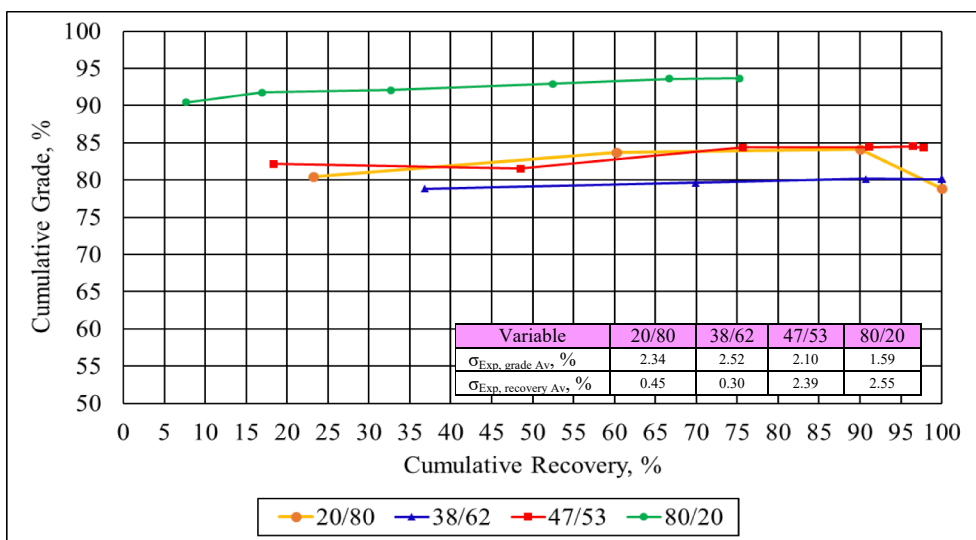
Fig. 8. Cumulative Recovery versus Cumulative Grade for Graphite Concentrates from Flotation Tests Using Different Compositions Tested. (Using NMC-111 Cathode Material and A-88 as Frother).

3.2.2. Flotation trials with different graphite/oxide compositions

The first series of results showed that for the composition 47 % graphite and 53 % lithium metal oxides that this can be separated using flotation under optimized conditions. In this second series of tests, the composition is varied between graphite/oxide compositions from 20 wt % / 80 wt% to 80 wt% / 20 wt% using the oxide NMC-111 cathode material as representative sample of the three oxides from the preceding section. The processing conditions are again those provided in Table 2.

The experimental results in Fig. 6 shows that for any composition below 47 wt% graphite (the top 3 green curves) give a graphite recovery above 97 %. The fourth and lowest of the green curves corresponding to 80 wt% graphite has much slower kinetics. Similarly, for the same 3 compositions, there is a low recovery of oxides in the concentrate (less than 16.35 %).

Fig. 7 indicates similar entrainment factors and are not strongly affected by composition, where the 80 % graphite is significantly lower. Fig. 8 shows that the cumulative grade for the 80 % metal oxide composition is above 90 % for all the flotation times, this indicates that a cleaner stage after a rougher stage is can be beneficial in order to get a high-grade graphite product. However, for the other three compositions,

the cumulative grade is around 80 % and presented in a narrow band between 80 and 85 %.

Fig. 8 shows that the cumulative grade for the three compositions below 47 % graphite all produce a cumulative grade of around 80 %; the implication of this will be discussed in the next section.

4. Discussion

The Cumulative Separation Efficiency (CSE) defined by equation (6) gives the separation after 8 min of flotation. The results from experiments conducted without any collector reagent added are provided in the Supplementary File and key results shown in Fig. 9.

CSE results indicate similar values for the oxides LCO and NMC with around 80 % of separation efficiency. For the oxide NCA, values are higher, around 90 %. When these materials are treated using kerosene as collector, a small improvement in this variable is noted for all oxides. This improvement can be understood considering the materials used in these tests are new and clean without any prior electrochemical treatment compared with spent commercial batteries after use due to solid electrolyte interface (SEI) formation during charging and discharging

Experiment	0 g/t	350 g/t	Δ S.E, %
Gp/LCO/A88	78.67	80.08	1.40
Gp/NMC/A88	80.55	81.40	0.85
Gp/NCA/Oct	89.93	90.16	0.23
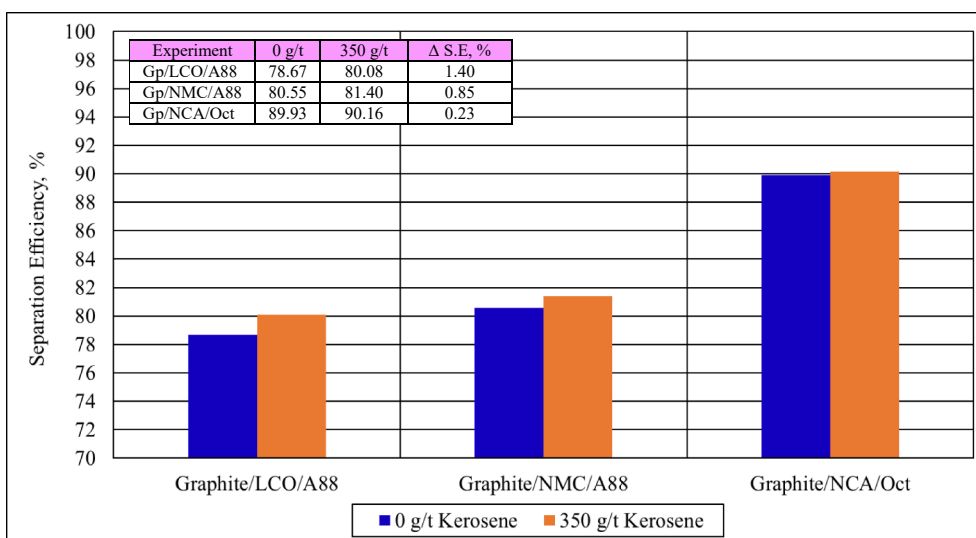
Fig. 9. Separation Efficiency versus Collector Dosage for Flotation Tests with and without Collector Addition.

Variable	LCO	NMC	NCA
Reagent	A88/K	A88/K	Oct/K
k, min^{-1}	0.40	0.63	0.59
RI, %	97.32	98.00	100
θ, min	0.30	0.05	0.36
R^2	0.991	0.996	0.986
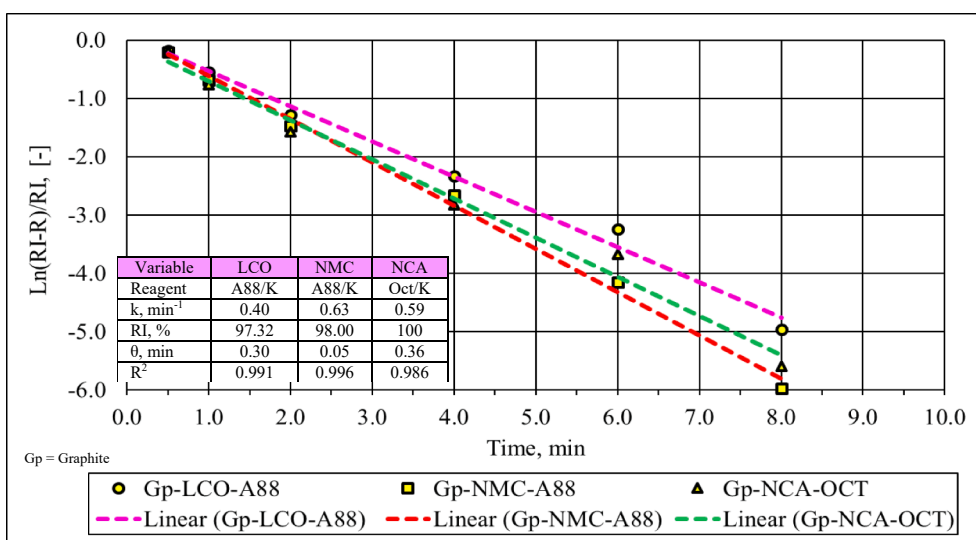
Gp = Graphite

Fig. 10. First Order Rate Plot for Graphite for Each Oxide Tested.

processes (Peled et al. 2011 and Peled et al. 2017) [31,32].

Figs. 10 and 11 are obtained by fitting the graphite recovery (Fig. 10) and the oxide recovery (Fig. 11) to equation (8) in a logarithm form in order to obtain the rate of recovery as a function of time. The regression constants for the linear correlation for each case are given in the table within each figure. The data in Fig. 10 indicates fast flotation kinetics for graphite, where the fastest kinetics were for the mixture of Graphite/NMC using Aerofroth-88® as the frothing agent. The θ values for these experiments (equation (8)) indicate a small positive correction for graphite when it is floated. This correction usually means that the material being recovered (graphite) begins to float even before air is introduced. This phenomenon is common for naturally hydrophobic materials.

Similarly, Fig. 11 also shows a linear correlation for the rate of recovery of each oxide with low recoveries as indicated by the respective values of the Ultimate Recovery (RI), with the mixture of Gp/NCA having the lowest value. These results also indicate significantly slower kinetics for the mixture Gp/LCO using Aerofroth-88® as frother. The θ values for these experiments also indicate a small positive correction with time.

The Selectivity index (SI) is obtained from equation (9). The results

show similar behavior for LCO and NMC cathode materials. In contrast, SI values for the NCA oxide is around double the others. When these materials are treated using kerosene as collector, a small improvement in this variable is noted. The greatest improvement is reported for the mixture Graphite/LCO using Aerofroth-88® as frother - the smallest improvement is reported for the mixture Graphite/NMC using Aerofroth-88®.

The experimental entrainment factor is calculated from the linear correlations of oxide recovery versus water recovery (Fig. 4), and the data are shown in Fig. 13. When kerosene is used as the collector, the entrainment factor is reduced (by 15.69 % on average) for the mixtures of Graphite/LCO and Graphite/NMC. By contrast for the mixture Graphite/NCA, this value is increased by 60 %, but is still a very low value of entrainment when compared with the other two oxides.

From all of these results, the combination Graphite/NCA would appear to be significantly easier to separate compared with the other two oxides. This is particularly evident from the higher separation efficiency, separation index, and entrainment factor (Figs. 9, 12 and 13). A possible explanation could relate to the particle size. The LCO/NMC cathode materials both have a similar particle size D_{50} between 5.0 and 7.5 μm, whereas the NCA material presents a D_{50} of 12 μm. This factor is
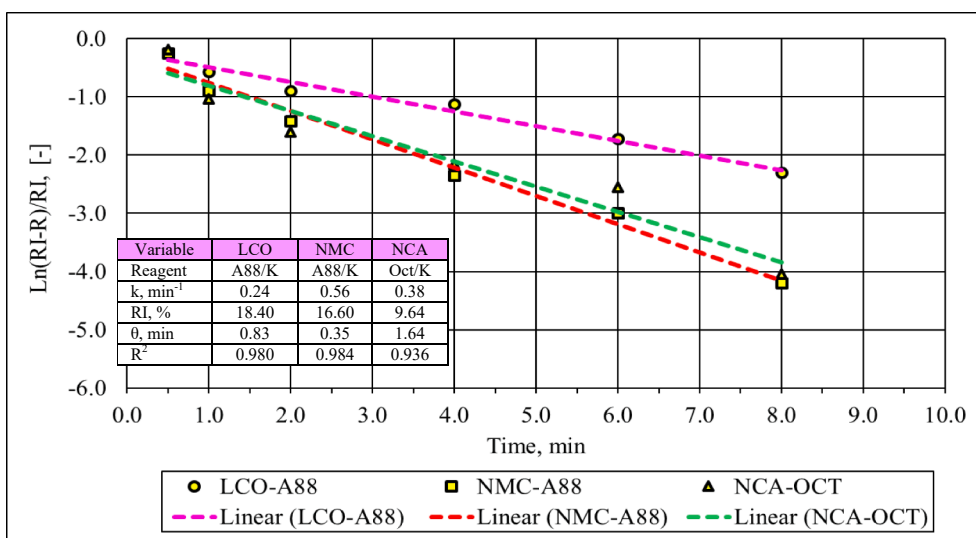
Fig. 11. First Order Rate Plot for Each Oxide Tested.

Variable	LCO	NMC	NCA
Reagent	A88/K	A88/K	Oct/K
k, min^{-1}	0.24	0.56	0.38
RI, %	18.40	16.60	9.64
θ, min	0.83	0.35	1.64
R^2	0.980	0.984	0.936
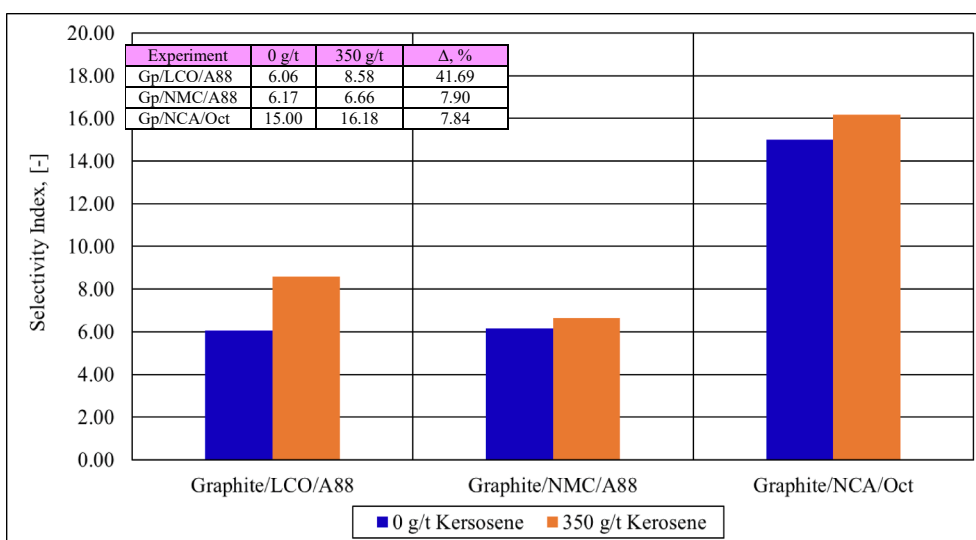
Fig. 12. Selectivity Index versus Collector Dosage for Each Oxide Tested.

Experiment	0 g/t	350 g/t	Δ, %
Gp/LCO/A88	6.06	8.58	41.69
Gp/NMC/A88	6.17	6.66	7.90
Gp/NCA/Oct	15.00	16.18	7.84

further explored by plotting the entrainment factor versus particle size in Fig. 14. This shows a strong correlation between the entrainment factor and particle size for each cathode material for experiments with collector (350 g/t) and without collector (0 g/t).

In these experiments the use of kerosene as a collector produces only a relatively small improvement in the graphite recovery. This may be due to the clean high purity graphite particles used in these experiments. The main purpose of this paper is to provide data on a model system for comparison with the real spent battery system. It is speculated from these results and the work published previously by Kim et al. (2004) and Vanderbruggen et al. (2021) [33,34] that the benefits of a collector in the flotation of the commercial spent graphite material may be more significant. Therefore, it is useful to have both sets of data collector/ collectorless results as points of comparison.

The final point relates again to the value of this work as a model system. These results indicate that if the spent battery material can be completely liberated from the binder materials, so that they have an effective liberation factor of 1.0 (same as this work) (Pitard 1993) [35], then flotation should be able to achieve separation efficiencies of 80–90 % which indicates that commercial grades of both graphite and lithium metal oxides could be achieved in 2–3 separation stages. However, in the

case of real systems where graphite and lithium metal oxides are mixed and agglomerated, they present a liberation factor ranging between 0.12 and 0.91 for graphite and 0.30–0.86 for the lithium metal oxides, depending on the size fraction analysed (Vanderbruggen et al. 2021) [36]. Therefore, the binder removal step needs special attention in order to maximise the liberation factor of these materials.

Considering the composition experiments, the composition 47 % graphite and 53 % oxides presented in the first series of results is shown by the second set of tests to be representative of the results of all the compositions tested from 47 % including the 38 % and 20 % graphite results. The 47 % Gp and 53 % Oxide composition is a more conservative composition from a flotation perspective, than the 38/62 composition due to the slightly slower kinetics, but they still demonstrate a high separation efficiency in the flotation process and this demonstrates that under these processing conditions, graphite and oxides can be separated efficiently with a low/moderate entrainment of oxides in the concentrate. However, the cumulative grade (Fig. 8) is a particularly important result, because it shows that for any feed concentration at or below 47 % graphite, the graphite grade after one stage of flotation can be expected to be around 80 %. The experiment result using 80 % graphite in the feed indicates that a second stage of flotation will improve the graphite grade

Experiment	0 g/t	350 g/t	Δ, %
Gp/LCO/A88	0.34	0.29	-14.71
Gp/NMC/A88	0.30	0.25	-16.67
Gp/NCA/Oct	0.10	0.16	60.00
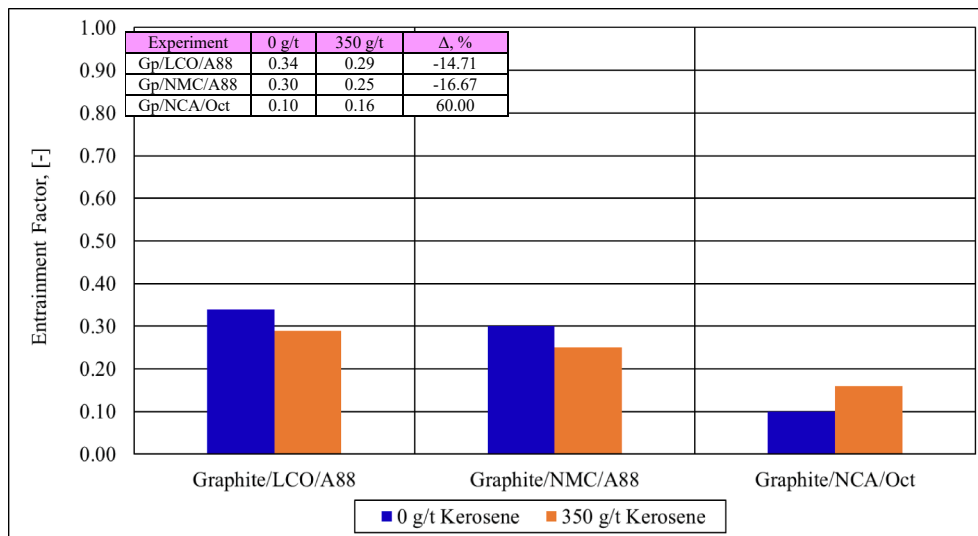
Fig. 13. Entrainment Factor versus Collector Dosage for Each Oxide Tested.
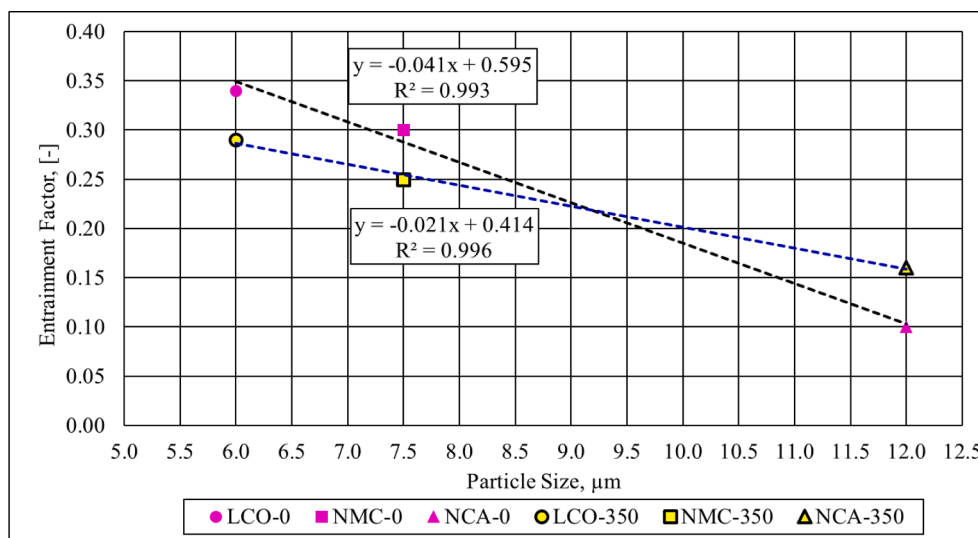
Fig. 14. Entrainment Factor versus Particle Size D_{50} for Each Oxide Tested. (0 and 350 Represents the Collector Dosage).

to above 90 % in the concentrate.

5. Conclusions

In this experimental study, synthetic mixtures of anode-grade graphite and cathode-grade lithium metal oxides have been separated by froth flotation. Good separation results were achieved in just one batch flotation stage for all three commonly-used lithium metal oxides. The main conclusions from this study are the following:

(1) The flotation response of completely liberated and pure LCO, NMC and NCA cathode materials from high purity graphite is relatively similar and all are able to be separated efficiently from the graphite in one flotation stage.

(2) The entrainment factor is strongly correlated with the particle size for each oxide tested. In terms of the oxide recovery, NCA material shows the best separation efficiency with the lowest oxide content in concentrates. A possible explanation is NCA's larger particle size leading to a significantly lower degree of entrainment.

(3) The entrainment plots for every cathode material evaluated show a high correlation between the water recovery and the oxide recovery, which confirms that entrainment by water recovery is the main mechanism for oxides reporting to the graphite concentrate.

(4) From the three different frothing reagents evaluated, Aerofroth-88 shows good results for mixtures of graphite with LCO and/or NMC in terms of both the flotation kinetics for graphite and a low oxide recovery in the concentrate. For mixtures of graphite and NCA, 2-octanol is the best frother.

(5) Different mixtures of graphite and lithium metal oxide were tested and results for 47 % graphite or lower (38 % or 20 %) gave similar results. The 47 % data had slightly slower kinetics, but still high recoveries (over 97 %) for graphite and low recoveries for oxide tested (less than 17 %) for a single flotation stage.

(6) The compositions results show that>80 % purity of graphite in the concentrate can be achieved in a single flotation stage for any feed grade at or below 50 % graphite. Flotation experiments with graphite grades over 80 % in feed can result in a graphite concentrate with grades>90 %. This suggests the use of additional flotation stages are required to produce high purity graphite concentrates.

This study shows that if the spent LIBs materials can be fully liberated, a high degree of separation can be achieved in just one flotation stage. Therefore, these results provide a strong basis for continuing the development of a flotation process, as a low energy and low chemical intensity separation process, for the recovery of the metal oxides and graphite materials used in spent LIBs.

CRediT authorship contribution statement

Luis Verdugo: Conceptualization. **Lian Zhang:** Supervision. **Kei Saito:** Supervision. **Warren Bruckard:** Methodology. **Jorge Menacho:** Methodology. **Andrew Hoadley:** Supervision.

Declaration of Competing Interest

The authors declare the following financial interests/personal relationships which may be considered as potential competing interests: Luis Verdugo reports equipment, drugs, or supplies was provided by Solvay Interox Pty Ltd. Luis Verdugo reports writing assistance was provided by De Re Metallica Ingenieria SpA.

Data availability

Data will be made available on request.

Appendix A. Supplementary material

Supplementary data to this article can be found online at https://doi.org/10.1016/j.seppur.2022.121885.

References

[1] National Blue Print for Lithium Batteries 2021-2030, Office of Energy Efficiency & Renewable Energy, US Government, Executive Summary, June 2021. Available online: https://www.energy.gov/sites/default/files/2021-06/FCAB%20National%20Blueprint%20Lithium%20Batteries%200621_0.pdf (accessed on 16 March 2022).

[2] N. Boxall, S. King, K. Cheng, Y. Gumulya, W. Bruckard, A. Kaksonen, Urban Mining of Lithium-Ion Batteries in Australia: Current State and Future Trends, Miner. Eng. 128 (2018) 45–55.

[3] M. Wentker, M. Greenwood, J. Leker, A Bottom-up Approach to Lithium-Ion Battery Cost Modeling with a Focus on Cathode Active Materials, Energies 12 (2019) 504.

[4] J. Jacoby, It's Time to Get Serious About Recycling Lithium-Ion Batteries, Chemical & Engineering News, 97, 28, July 15, 2019. Available online: https://cen.acs.org/materials/energy-storage/time-serious-recycling-lithium/97/i28 (accessed on 23 March 2022).

[5] K. Vuorilehto, Materials and function, in: R. Korthauer (Ed.), Lithium-Ion Batteries: Basics and Applications, Springer, Berlin, Heidelberg, 2018.

[6] J. Zhang, J. Qiao, K. Sun, Z. Wang, Balancing particle properties for practical lithium-ion batteries, Particuology 61 (2022) 18–29.

[7] Y. Zhao, O. Pohl, A.I. Bhatt, G.E. Collis, P.J. Mahon, T. Rüther, A.F. Hollenkamp, A review on battery market trends, second-life reuse, and recycling, Sustain. Chem. 2 (1) (2021) 167–205.

[8] N. Nitta, F. Wu, J. Tae Lee, G. Yushin, Li-ion battery materials: present and future, Mater. Today 18 (5) (2015) 252–264.

[9] K. Gallagher, P. Nelson, 6 - Manufacturing Costs of Batteries for Electric Vehicles, in: Gianfranco Pistoia (Ed.), Lithium-Ion Batteries, Elsevier, 2014, 97–126.

[10] L. Gaines, J. Sullivan, A. Burnham, Paper No. 11-3891 Life-Cycle Analysis for Lithium-Ion Battery Production and Recycling, Transportation Research Board 90th Annual Meeting, Washington, DC, 2011.

[11] K. Winslow, S. Laux, T. Townsend, A review on the growing concern and potential management strategies of waste lithium-ion batteries, Resour. Conserv. Recycl. 129 (2018) 263–277.

[12] F. Tinu-Ololade, A. Lipson, J. Durham, H. Pinegar, D. Liu, L. Pan, Direct Recycling of Blended Cathode Materials by Froth Flotation, Energy Technol. 9 (10) (2021) 2100468.

[13] C. Hanisch, T. Loellhoeffel, J. Diekmann, K. Markley, W. Haselrieder, A. Kwade, Recycling of Lithium-Ion Batteries: A Novel Method to Separate Coating and Foil of Electrodes, J. Clean. Prod. 108 (Part A) (2015) 301–311.

[14] Y. He, X. Yuan, G. Zhang, H. Wang, T. Zhang, W. Xie, L. Li, A critical review of current technologies for the liberation of electrode materials from foils in the recycling process of spent lithium-ion batteries, Sci. Total Environ. 766 (2021), 142382.

[15] G. Parks, Aqueous Surface Chemistry of Oxides and Complex Oxide Minerals, Adv. Chem. 67 (1967) 121–160.

[16] P. Somasundaran, Zeta Potential of Apatite in Aqueous Solutions and Its Change During Equilibration, J. Colloid Interface Sci. 27 (4) (1968) 659–666.

[17] W. Trahar, L. Warren, The Flotability of Very Fine Particles — A Review, Int. J. Miner. Process. 3 (2) (1976) 103–131.

[18] B. Shahbazi, B. Rezai, S. Koleini, Bubble-Particle Collision and Attachment Probability on Fine Particles Flotation, Chem. Eng. Process. Process Intensif. 49 (6) (2010) 622–627.

[19] V. Kirjavainen, Mathematical Model for The Entrainment of Hydrophilic Particles in Froth flotation, Int. J. Miner. Process. 35 (1992) 1–11.

[20] V. Kirjavainen, Review and Analysis of Factors Controlling the Mechanical flotation of Gangue Minerals, Int. J. Miner. Process. 23 (1996) 33–53.

[21] Barry A. Wills, Tim Napier-Munn, Chapter 1 - Introduction, Editor(s): Barry A. Wills, Tim Napier-Munn, Wills' Mineral Processing Technology, 7th Edition, Butterworth-Heinemann, 2005, Pages 1-29.

[22] O. Savassi, D. Alexander, J. Franzidis, E. Manlapig, An Empirical Model for Entrainment in Industrial Flotation Plants, Miner. Eng. 11 (3) (1998) 243–256.

[23] W. Zhang, J. Nesset, R. Rao, J. Finch, Characterizing Frothers Through Critical Coalescence Concentration (CCC)95-Hydrophile-Lipophile Balance (HLB) Relationship, Minerals 2 (2012) 208–227.

[24] P. Kowalczuk, S, Determination of Critical Coalescence Concentration and Bubble Size for Surfactants Used as Flotation Frothers, Ind. Eng. Chem. Res. 52 (2013) 11752–11757.

[25] D. Wang, Flotation Reagents: Applied Surface Chemistry on Minerals Flotation and Energy Resources Beneficiation, Volume 1: Functional Principle, Metallurgical Industry Press, Beijing, China, 2016, 382pp.

[26] M. Xu, Modified Flotation Rate Constant and Selectivity Index, Miner. Eng. 11 (3) (1998) 271–278.

[27] G.E. Agar, J.J. Barrett, The Use of Flotation Rate Data to Evaluate Reagents, CIM Bull. 76 (1983) 157–162.

[28] W. Bauer, F. Çetinel, M. Müller, U. Kaufmann, Effects of pH control by acid addition at the aqueous processing of cathodes for lithium ion batteries, Electrochim. Acta 317 (2019) 112–119.

[29] I. Shkrob, J. Gilbert, P. Phillips, R. Klie, R. Haasch, J. Bareño, D. Abraham, Chemical Weathering of Layered Ni-Rich Oxide Electrode Materials: Evidence for Cation Exchange, J. Electrochem. Soc. 164 (2017) A1489.

[30] Z. Konopacka, J. Drzymala, Types of particles recovery—water recovery entrainment plots useful in flotation research, Adsorption 16 (2010) 313–320.

[31] E. Peled, S. Menkin, Review—SEI: Past, Present and Future, J. Electrochem. Soc. 164 (7) (2017) A1703–A1719.

[32] E. Peled, D. Golodnitsky, J. Penciner, The Anode/Electrolyte Interface, in: C. Daniel, J.O. Besenhard (Eds.), Handbook of Battery Materials, 2011.

[33] Y. Kim, M. Matsuda, A. Shibayama, T. Fujita, Recovery of LiCoO2 from Wasted Lithium Ion Batteries by Using Mineral Processing Technology, Resour. Process. 51 (1) (2004) 3–7.

[34] A. Vanderbruggen, J. Sygusch, M. Rudolph, R. Serna-Guerrero, A Contribution to Understanding the Flotation Behavior of Lithium Metal Oxides and Spheroidized. Graphite for Lithium-ion Battery Recycling, Colloids Surf. A: Physicochem. Eng. Aspects 626 (2021), 127111.

[35] F. Pitard, Pierre Gy's Sampling Theory and Sampling Practice: Heterogeneity, Sampling Correctness, and Statistical Process Control, Second Edition, CRC Press, Boca Raton, USA, 1993, p. 488.

[36] A. Vanderbruggen, E. Gugala, R. Blannin, K. Bachmann, R. Serna-Guerrero, M. Rudolph, Automated Mineralogy as a Novel Approach for the Compositional and Textural Characterization of Spent Lithium-Ion Batteries, Miner. Eng. 169 (2021), 106924.

[37] J. Liu, H. Wang, H.u. Tingting, X. Bai, S. Wang, W. Xie, J. Hao, Y. He, Recovery of LiCoO2 and graphite from spent lithium-ion batteries by cryogenic grinding and froth flotation, Miner. Eng. 148 (2020), 106223.

[38] Y.u. Jiadong, Y. He, Z. Ge, H. Li, W. Xie, S. Wang, A promising physical method for recovery of LiCoO2 and graphite from spent lithium-ion batteries: Grinding flotation, Sep. Purif. Technol. 190 (2018) 45–52.

[39] X. Yang, A. Torppa, K. Kärenlampi, Evaluation of Graphite and Metals Separation by Flotation in Recycling of Li-Ion Batteries, Mater. Proc. 5 (2021) 30.

[40] R. Zhan, Z. Oldenburg, L. Pan, Recovery of active cathode materials from lithium-ion batteries using froth flotation, Sustain. Mater. Technol. 17 (2018) e00062.